

Luminescence quenching of ordered π -conjugated molecules near a metal surface: Quaterthiophene and PTCDA on Ag(111)

W. Gebauer,¹ A. Langner,¹ M. Schneider,¹ M. Sokolowski,^{1,2,*} and E. Umbach¹

¹*Experimentelle Physik II, Universität Würzburg, Am Hubland, D-97074 Würzburg, Germany*

²*Institut für Physikalische und Theoretische Chemie der Universität Bonn, Wegelerstraße 12, D-53115 Bonn, Germany*

(Received 9 April 2003; revised manuscript received 17 February 2004; published 30 April 2004)

Photoluminescence (PL) spectra were measured for highly ordered films of two planar π -conjugated molecules [quaterthiophene and 3,4,9,10-perylenetetracarboxylicacid-dianhydride (PTCDA)], which were both grown on a Ag(111) surface with thicknesses varied between 1 and 30 monolayers. For both molecules the PL is quenched below the detection limit for two-layer-thick films and increases very steeply for thicker films. These results cannot be explained within the classical image dipole theory, but demonstrate the presence of ultrafast, nonradiative short-range decay processes, such as charge delocalization and tunneling. It is effective for the first chemisorbed molecular layer *and* the second molecular layer on top of the first. Implications of these findings for luminescence experiments on organic films in close contact to metal surfaces are discussed.

DOI: 10.1103/PhysRevB.69.155431

PACS number(s): 78.55.Kz

I. INTRODUCTION

The influence of a metal surface on the lifetime of an oscillating dipole has been the subject of considerable experimental and theoretical efforts since the first reports on this topic.¹ During recent years the optical properties of thin films of π -conjugated molecules have attracted enormous research interest because of their potential applications, e.g., in organic light emitting devices or solar cells,² and since it has become possible to grow thin films of various π -conjugated molecules with long-range order on crystalline metal surfaces.³ In this context the fundamental question of the influence of the contacts, or, speaking more generally, the quenching of an optical excitation near a metal surface, has again emerged. Experimental results have been preferentially discussed in the framework of the so-called classical theory, mainly developed by Chance, Prock, and Silbey.⁴ For distances to the surface much smaller than the dipole wave length, nonradiative, Förster-like energy transfer to the metal image dipole occurs and quenches the luminescence. This leads to a transfer rate increasing with z^{-3} , whereby z is the distance of the dipole to the surface.⁴

A large number of experiments were performed on thin layers of dye molecules separated from metal surfaces by spacer layers and have supported the classical theory down to very small distances.⁵ However, the situation in which a few layers of luminescent molecules are adsorbed directly on a microscopically well-defined metal surface, i.e., a surface that is atomically flat and chemically clean, has been much less thoroughly investigated.^{6,7} Nevertheless, this case is of high interest because deviations from classical theory due to quantum-mechanical effects, e.g., influences of the substrate on the electronic structure of the individual molecules and especially of the chemisorptive molecule-substrate bonding on the energy transfer mechanism, are most likely for the very first molecular layers at the metal interface.

One main difficulty of unambiguous experimental investigations on the luminescence in the first-few-layer thickness regime of organic films on metal surfaces is the achievement

of a sufficiently high structural order at the organic/metal interface. The preparation of a well-defined, clean, and atomically smooth metal surface and a high and reproducible structural order in the organic film itself is inevitable, because only in this case one can be sure that the observed interface properties are not determined by impurities and/or (substrate-induced) structural defects, e.g., grain boundaries, which act as traps and/or nonradiative decay channels. Moreover, for the first molecular layers, structural order is relevant, since the local bonding geometry of a molecule on the metal determines the overlap of molecular orbitals and electronic states of the substrate, which is decisive for the resulting rates of charge or energy transfer. In addition, the structural order within the film is of essential importance, because it determines the intermolecular overlap and thus the type and velocity of exciton migration within the film. Conclusively, large differences in transfer rates are to be expected for nominally identical films but with interfaces of different structural order.

To our knowledge, luminescence quenching of π -conjugated molecules on a metal surface has so far not been subject to detailed experiments as described above. Either the film thicknesses were far beyond the few-layer-thickness regime, or the metal surfaces were rough and structurally not defined,⁷ or the films themselves were disordered or even amorphous.^{6,7} From line broadening in electron loss spectroscopy for pyrazin on Ag(111), Avouris and Demuth deduced ultrashort lifetimes of the excited states in the first and second monolayer. However, neither the luminescence nor the structural order were measured.⁸

The intention of the experiments reported here was to investigate the luminescent decay for the singlet exciton states of π -conjugated molecules in the few-layer-thickness regime after a detailed precharacterization using various surface analytical methods and with a concomitant control of the structural order by low energy electron diffraction (LEED). We report data measured for two different planar model molecules, namely quaterthiophene (4T) and 3,4,9,10-perylenetetracarboxylicacid-dianhydride [PTCDA (see Fig. 1)], in order to demonstrate that the ob-

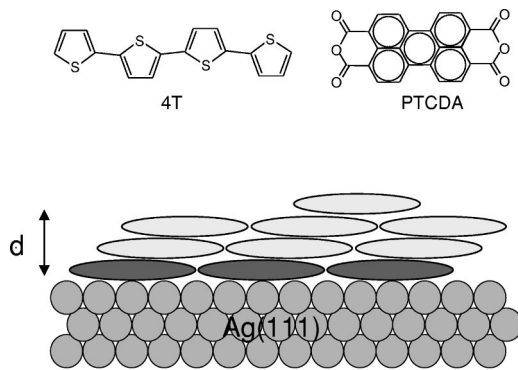


FIG. 1. Schematic cross section of the investigated films on the Ag(111) surface. The molecules are viewed perpendicular to the plane of the π systems. The molecules were either 4T or PTCDA, the structure formulas of which are shown at the top. The nominal film thickness is denoted as d . The thickness of one molecular layer corresponds to 3.6 and 3.2 Å for 4T and PTCDA, respectively. The gray shading of the first layer indicates its specific electronic structure with respect to layers farther away from the interface due to chemisorption. For further details, see text.

served interface quenching of the luminescence appears to be a general phenomenon for this type of chemisorbed organic molecules on metal surfaces. The focus of our work is, however, on the 4T films. The optical spectra of PTCDA (Refs. 9–11) will be reported and discussed in detail elsewhere.¹²

The S_0 - S_1 transitions of both molecules are π - π^* highest occupied molecular orbital–lowest unoccupied molecular orbital (HOMO-LUMO) transitions, with energies of 2.6 eV and 2.1 eV for 4T and PTCDA, respectively.^{13,9} Both molecules are chemisorbed on the Ag(111) surface^{14,15} with the molecular planes parallel to the surface, as schematically shown in Fig. 1. This is known from the dichroism of near-edge x-ray-absorption spectroscopy data (NEXAFS) (Ref. 16) and the absence of in-plane modes in Fourier transform infrared (FTIR) spectra.¹⁷ In PTCDA multilayers, the planar orientation is strictly maintained,¹⁶ whereas a small tilting of the molecular planes by about 30° is observed for 4T multilayers.¹⁸

The bonding of the molecules to the surface involves occupied π and unoccupied π^* orbitals of the molecules, located symmetrically above and below the molecular planes, and mainly Ag $4d$ - and $5s$ -derived states. The chemisorptive character of the bonding is most obvious from chemical shifts observed for the monolayer in comparison to physisorbed multilayers, e.g., in ultraviolet photoemission spectroscopy,^{14,15} NEXAFS,¹⁸ FTIR,¹⁷ and high-resolution EELS (HREELS) data.¹⁹ As a consequence of the chemical bonding to the Ag, the electronic structure of the monolayer differs from that of the multilayers adsorbed on top of the monolayer. In Fig. 1 we have indicated this by a heavier gray shading of the monolayer. As a consequence, the S_0 - S_1 transition energies are strongly modified for the monolayer. For instance, for PTCDA on Ag(111) the S_0 - S_1 transition of the monolayer was measured by HREELS and found at 360 meV, i.e., significantly below the S_0 - S_1 transition of multilayers at 2.1 eV.¹⁹ Due to this chemical modification of the monolayer, the second layer on top feels a local environment

which differs from that of molecules farther away from the interface. This can be derived, e.g., from the fact that the thermal desorption peak for the second layer of PTCDA films is separated from the multilayer peak²⁰ and from differences in the Raman modes of second and higher layers.²¹

II. EXPERIMENT

Photoluminescence (PL) and concomitant LEED measurements were carried out in one ultrahigh-vacuum system. The Ag(111) surfaces were prepared by sputter/annealing cycles and checked by LEED using standard procedures. The films of both molecules were grown by vapor deposition onto the Ag(111) substrate held at ~ 300 K and at rates of ~ 1 Å/min.

Especially, these small deposition rates allowed the deliberate preparation of films of few monolayers (ML) thickness. The nominal film thicknesses (d) were monitored by a quartz microbalance, which was calibrated to the number of monolayers by thermal desorption spectroscopy and LEED as follows: In the case of 4T, we exploited the fact that the monolayer (= 1 ML) does not desorb from the surface, due to chemisorption, as observed by x-ray photoemission spectroscopy.¹⁷ Thus we calibrated the reading of the quartz microbalance to 1 ML for the maximal deposited film thicknesses, which does not yield a thermal desorption signal. In addition, we used the change of the LEED pattern for the completion of the second monolayer (see below) as an additional calibration point (see Sec. III A below).

For PTCDA, we also used the above-noted procedure. However, thermal desorption spectra of PTCDA also show a well separated and saturating peak belonging to the second PTCDA layer,²⁰ which we additionally used to calibrate the film thickness. The integral under the “second-layer desorption peak” was normalized to 1 ML for PTCDA. (We note that for 4T the difference in binding energies between the second and third monolayer is too small for the second monolayer peak to be separated from the multilayer desorption peak.¹⁷) We reckon that the overall accuracy of the so-determined film thicknesses is about 10% for both molecules (see Fig. 3, below).

For optical spectroscopy, the sample was positioned into a special glass cylinder, standing out from one end of the chamber, which allowed us to bring a lens for collection of the luminescent light close to the sample. The light was analyzed with a monochromator (1.0 m focal length, $f\# = 8.6$), using a holographic grid with 1200 lines/mm. A cooled photomultiplier (Hamamatsu R2949, -30 °C) and single-photon counting was used. The PL spectra were measured at about 25 K for 4T and 335 K for PTCDA, using a broadband uv excitation with a Xe lamp [$\lambda = (400 \pm 20)$ nm] or an Ar⁺ laser ($\lambda < 365$ nm) for 4T, and an Ar⁺ laser at 488 nm for PTCDA. The PL measurements for PTCDA were performed at a temperature close to the preparation temperature (~ 300 K) in order to save time. This was justified, since additional measurements at low temperature did not reveal significant differences concerning the quenching. In order to measure the absorption spectra of 4T, photoluminescence excitation spectra (PLE) were recorded with a dye laser (cou-

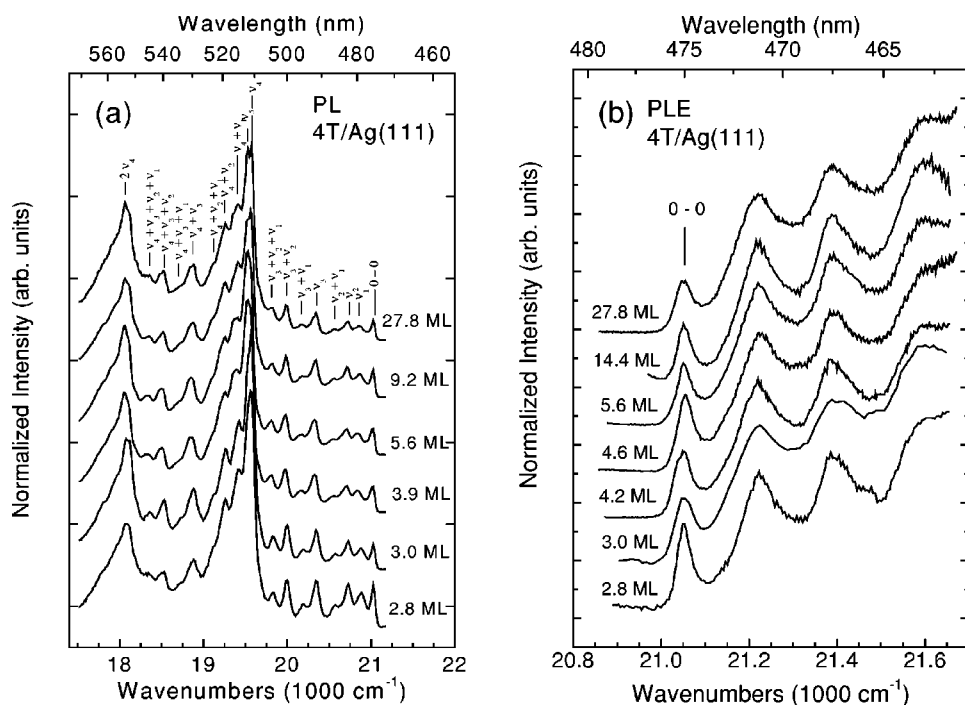


FIG. 2. Optical spectra of highly ordered 4T films on Ag(111) as a function of the film thickness given in the number of monolayers (ML). (a) Photoluminescence (PL) spectra (normalized at the strongest line ν_4 at $19\,500\text{ cm}^{-1}$). The fundamental vibronic modes and combinations thereof are indicated. (b) Photoluminescence excitation (PLE) spectra (normalized at the line at $21\,220\text{ cm}^{-1}$). Note the strong expansion of the wave-number axis in (b) with respect to (a).

marin 47) and detection of the strongest vibronic mode of the PL spectra at 530 nm (see Fig. 2, below). The uncertainty of the wave numbers in the PLE spectra due to a thermal drift of the dye laser is at most $\pm 15\text{ cm}^{-1}$.

III. RESULTS AND DISCUSSION

A. Film structures and morphologies

Before we turn to the optical data, we give a brief summary of the structural and morphological properties of our film, with particular emphasis on new aspects, relevant for our optical investigations. For both molecules the monolayers and multilayers are laterally ordered, which is deduced from LEED patterns with sharp spots due to lateral domain sizes larger than 300 \AA . The details of the lateral order of the 4T monolayer and 4T multilayers on Ag(111) were reported in Refs. 13 and 18. Remarkably, the monolayer LEED pattern is observed as long as the deposited amount of 4T molecules corresponds to not more than two monolayers. If further material is deposited, the pattern changes irreversibly to the multilayer LEED pattern, which is observed for all films above a thickness of two layers. The coverage of this structural phase transition was calibrated carefully, and then the phase transition was used to discriminate between 4T films of fewer and more than two layers thickness.

Deposition of more than two layers at a substrate temperature of about 300 K (as considered in the present work) leads to a 4T LEED pattern which was denoted as the β phase in Ref. 18. The corresponding optical spectra were discussed in Ref. 13. In the present work, we observed a second multilayer LEED pattern (for nominally identical preparation parameters) which is similar, but not identical to, the earlier LEED pattern of the β phase.¹⁸ So far we have not been able to figure out which preparation parameter decides between the growth of these two multilayer phases. Both

phases are likely to be polymorphic structures of 4T on Ag(111) with very similar free enthalpies. The optical spectra of both phases were nevertheless identical. In the following, we will denote them as the β_1 and β_2 phase of 4T. From packing considerations,²² we estimated the thickness of a 4T layer in multilayers as 3.6 \AA .

The monolayers and multilayers of PTCDA films on Ag(111) exhibit a lateral order which is very close to that of (102) PTCDA bulk planes.^{23,24} The thickness of one PTCDA layer can be thus estimated from the (102) layer spacing as 3.2 \AA .²⁵ For films grown at room temperature (as considered here), the stacking of the (102)-like layers in the direction perpendicular to the surface appears to be not unique, since x-ray-diffraction results indicate a mixture of domains with a stacking corresponding to the α or β bulk phase of PTCDA.²⁴ Optical spectra of PTCDA films on Ag(111) vary significantly, if the substrate temperature for the preparation or the deposition rate is varied.⁹⁻¹² However, the photoluminescence spectra of PTCDA films grown at room temperature and measured at room temperature, which are considered here, did not show variations with the film thickness.

After 4T deposition, the LEED spots of the substrate are attenuated. Therefore, 4T films on Ag(111) must grow in a layer-by-layer (Frank-van der Merwe) mode, at least for the first two to three layers. For thicker layers the growth may not occur in an ideal layer-by-layer mode. If cluster growth would occur already from the second or third layer onward (Stranski-Krastanov growth mode), the LEED spots of the substrate would be attenuated only to a certain level. The formation of a closed second layer of 4T is also supported by the optical data themselves (see below). However, we cannot exclude that the growth proceeds with more than one open layer, especially if the films become thicker than about three layers.

The morphology of PTCDA films on Ag(111) could be directly observed by photoemission microscopy.²⁶ After closure of the second layer, film growth proceeds with more than one open layer. However, cluster formation, as observed at 400 K,²⁶ does not occur at 300 K. In conclusion, at least two closed layers form on the substrate for 4T and PTCDA, and deviations from ideal layer-by-layer growth may occur from the third or fourth layer onward, similar to the growth scenario reported in Ref. 27.

B. Absence of luminescence of the first two layers

The most important result is the absence of any PL for films with thicknesses up to two monolayers. This finding holds for both molecules. The smallest film thickness for which PL was observed was 2.2–2.3 ML. A PL spectrum taken of a 2.8 ML 4T film is shown in Fig. 2(a). Several experiments in this thickness range all confirmed an onset of the PL at a thickness of more than 2 ML. Sometimes small luminescent spots were detected on the sample for 2-ML-thick films, but they were always directly related to macroscopic defects on the Ag(111) surface, e.g., scratches. This result also corroborates that the first 2 ML grow in a layer-by-layer mode and close before the third layer starts to grow, since otherwise PL would occur from molecules in the third layer, even for films with a nominal thickness below 2 ML. Conclusively, there must exist an ultrafast quenching process at the metal interface which suppresses the PL of not only the chemisorbed monolayer, but also of a *two-layer-thick* film.

The above result is in clear contrast to the earlier reported observation of PL from *disordered* films on metal surfaces down to the submonolayer thickness regime.⁶ Because the LEED experiments were always performed *after* the PL measurements, we can clearly rule out that 4T or PTCDA was desorbed, destroyed, and/or disordered during the PL experiment.

C. Optical spectra as a function of film thickness

From about 2.2 ML on, the PL yield increases sharply. At about 2.3 ML, 4T films show separated luminescent spots, which coalesce to a closed uniformly luminescent layer, if about one further layer of 4T, i.e., the third, is deposited. This also indicates that the third layer closes. Regardless of the film thickness, all obtained PL and PLE spectra exhibit the same highly resolved vibrational fine structure specific for undistorted 4T molecules,^{28,29} as demonstrated in Fig. 2. There are no indications for any additional lines evolving with increasing film thickness, revealing that all films consist of one homogeneous phase without any traps, as expected from their identical LEED patterns. In the PL spectra, the 0-0 transition is found at $21\,025 \pm 5 \text{ cm}^{-1}$ independent of thickness d . It is within 22 cm^{-1} in resonance with the 0-0 transition in the PLE spectrum, i.e., the peak at the smallest energy [see Fig. 2(b)]. The position of the 0-0 transition in the PLE spectrum is also constant as a function of thickness d within the error of the experiment even for the thinnest films (2.3 ML), for which we could measure the PLE spectra with sufficient signal-to-noise ratio.

Excitation just below the 0-0 transition did not lead to PL [see Fig. 2(b)], excluding shallow luminescent traps. The small linewidth (FWHM_{0-0} in $\text{PL} \leq 40 \text{ cm}^{-1}$) is a consequence of the high structural order, because for less-ordered films, e.g., prepared on less-defined surfaces, the vibrational lines are found to be strongly washed out due to inhomogeneous broadening.¹³

The only variations of the optical spectra of 4T which are observed for increasing thickness are changes in the relative intensities. For instance, in the PL spectra the intensity of the peaks to the right of the strongest peak ν_4 decreases with increasing thickness. This effect was already discussed in Ref. 13 as a consequence of the increasing intermolecular coupling of the excitons with an increasing number of molecular layers. A similar effect is also noted for the PLE (absorption) spectrum in Fig. 2(b), where the intensity of the 0-0 line decreases with respect to the lines at higher energies as a function of thickness. The details of this effect will be discussed elsewhere.³⁰

For PTCDA, the interpretation of the optical spectra has been a matter of discussion in recent years (see, e.g., Ref. 11 and references therein) and is more complicated than for 4T. In the present context, where the focus is on the luminescence yields, it is only important that we did not observe changes of the spectral shape with increasing film thickness, similar to the case of 4T.

D. Quantitative description of the luminescence yield

We now consider the PL yield quantitatively as a function of the film thickness (d). For this purpose we integrated the PL spectra over the wavelength range shown in Fig. 2(a), normalized the integrated intensity by the nominal film thickness d , and plotted this result as a function of d (Fig. 3). In the case of PTCDA, a spectrum of the clean Ag(111) sample was subtracted from the PL spectrum in order to correctly account for the luminescence background arising, e.g., from molecules which had unintentionally adsorbed from the residual gas on the inside of the glass cylinder around the sample. This was, however, necessary only for films of very low PL yield. The computed numbers [$\bar{\eta}(d)$] are proportional to the PL yield of a molecule *averaged* over the film thickness d . This determination of the PL yield is based on the assumption that the excitation probability, i.e., the electric field strength, is constant within the film, and, in particular, independent of the distance to the Ag(111) surface. This is well fulfilled because the wavelength is much larger than the layer thickness and one can estimate that the reflectivity of the 4T/Ag(111) interface is only $\sim 40\%$ at the excitation wavelength,³¹ and hence there is no sharp node of the electric field at the interface. Note that Fig. 3 is a double logarithmic plot. There is a significant scattering of the data points, which is caused by variations of the optical setup, e.g., focusing of the laser and the efficiency of collection of the luminescent light, and of course due to uncertainties in the film thickness. Nevertheless, the data demonstrate clearly the above-mentioned steep increase of $\bar{\eta}(d)$ between 2 and 10 ML for both molecules, and both phases of 4T. Figure 3 further reveals that $\bar{\eta}(d)$ is about constant above 10 ML.

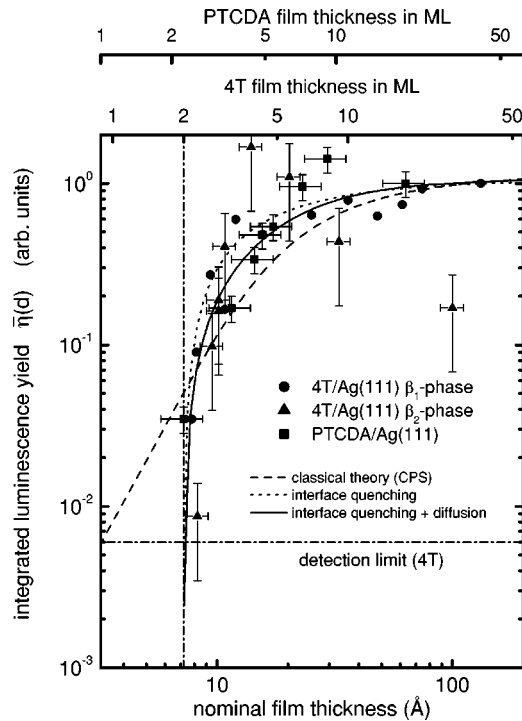


FIG. 3. Averaged PL yield [$\bar{\eta}(d)$] of 4T and PTCDA films on Ag(111) vs nominal film thickness d . The experimental data points were normalized to 1 at $d=65$ Å (PTCDA) and $d=110$ Å (4T), respectively; the theoretical curves were normalized at $d=100$ Å. The axis at the top of the figure displays the nominal film thickness in number of monolayers. Dashed line, expected $\bar{\eta}(d)$ behavior according to the classical theory. Short-dashed line, $\bar{\eta}(d)$ based on an ultrafast exciton decay at the organic/Ag(111) interface. Full line, as a dashed line, but also accounting for exciton diffusion [diffusion constant 10^{-5} cm² s⁻¹ (Ref. 43)]. Error bars due to variations in the optical setup and the determined film thickness are indicated. Since the error bars of the β_1 and β_2 phase are comparable, only those of β_2 are indicated, in order to avoid overloading of the figure. The experimental detection limit due to the signal-to-noise ratio of the detection system is indicated for 4T. For PTCDA, the detection limit is higher by about a factor of 3 due to the intrinsically lower luminescence yield of PTCDA compared to 4T.

In order to test whether the data can be described by the classical theory, we calculated $\bar{\eta}(d)$ using a transfer rate $k_{\text{nonrad}}=k_{\text{rad}}(d_0/z)^3$ (Ref. 4) and integrating over all emitters within the film,

$$\begin{aligned} \bar{\eta}(d) &= \frac{1}{d} \int_0^d \eta(z) dz \\ &= \frac{1}{d} \int_0^d \frac{k_{\text{radiative}}}{k_{\text{radiative}} + k_{\text{nonradiative}}} dz \\ &\propto \frac{1}{d} \int_0^d \frac{1}{1 + (d_0/z)^3} dz. \end{aligned} \quad (1)$$

Thereby we assumed $k_{\text{rad}}=\text{const}$, as is usually done.⁴ The best agreement with the experimental data is obtained for a characteristic quenching distance $d_0=12$ Å (Fig. 3, dashed line), a value which is roughly of the order of the value d_0

$=70$ Å that is calculated on the basis of the classical theory⁴ using the optical constants of Ag (Ref. 32) and the 4T film.³³ However, as is evident from Fig. 3, the “effective” slope of ~ 2.5 of the so-obtained model curve [$\bar{\eta}(d) \propto d^{-2.5}$] is too small to explain the steep decrease for $d < 30$ Å (see Fig. 3, long-dashed line). In particular, it would require the observation of luminescence of 4T well above our detection limit (dashed-dotted line) for thicknesses below $d \leq 2$ ML (Fig. 3), in contrast to our observation. In addition, the model curve predicts much smaller luminescence yields in the region of 10–30 Å than we actually observe. This is also true for higher reasonable exponents of k_{nonrad} (e.g., $k_{\text{nonrad}} \propto z^{-4}$),³⁴ or smaller values of d_0 , which we have systematically tested. Model calculations of $\bar{\eta}(d)$ for a nonideal layer-by-layer growth were also performed. However, unless we had an extreme cluster growth with a very high aspect ratio (height to width), which is completely inconsistent with our experimental data, these calculations also predict a luminescence for films between 1 and 2 ML, in contrast to the experimental data.

In conclusion, the discrepancy between the experimental data and the classical theory is serious. It can also not be lifted by reasonable variations of the position of the image plane or by accounting for exciton diffusion, since this tends to lower the slope of $\bar{\eta}(d)$ (see below). One may argue that dipole coupling to Ag surface plasmons at 3.6 eV plays an important role in the quenching process. However, this cannot be the case since calculations demonstrate that the plasmon is too far above the optical transition energies considered here to be effective.³⁵

Conclusively, we have evidence for a different quenching mechanism which is responsible for the luminescence rates of the first few layers and which in particular is very fast for the first two layers at the 4T/Ag and PTCDA/Ag interface. We propose that it is based on an ultrafast charge-transfer process from the *first two* molecular layers to the metal. Charge-transfer processes by rapid hole delocalization to the substrate through the chemical bonds or by tunneling from excited molecules to the substrate have been considered in surface science for a long time. They have been studied, e.g., in the framework of electron or photon stimulated desorption processes of adsorbed atoms or small molecules.³⁶ However, the importance of these mechanisms for the understanding of the PL in the few-layer regime of luminescent molecules on metallic substrates was not discussed so far and studied in detail. We will do this in the following and demonstrate that it explains our findings consistently.

E. Modeling the interface quenching

For the *first* layer, it is important to realize that the frontier orbitals HOMO and LUMO which are involved in the S_0 - S_1 excitation are strongly modified through the formation of bonds between the molecular π -orbitals and the Ag(111) surface. As noted at the beginning, the S_0 - S_1 transition of the monolayer can be directly observed by HREELS. In the case of PTCDA, the S_0 - S_1 transition of the monolayer is at rather small energies [0.36 eV (Ref. 19)] and falls below the range of the detected optical spectrum. We assume that the situa-

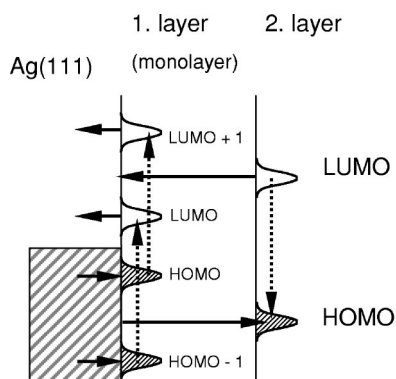


FIG. 4. Schematic energy diagram of the frontier orbitals in the first two molecular layers. The full arrows indicate resonant charge-transfer processes. The dashed arrows illustrate exciton transfer from the second to the first layer by Coulombic field coupling (perhaps involving internal conversion). For further details, see text.

tion for 4T is similar, although the energetic shift of the S_0 - S_1 transition to lower energies may be smaller due to a weaker surface bonding. A schematic diagram of the corresponding single-particle electronic states for the first two layers is shown in Fig. 4. Thereby we have also included the (chemically modified) LUMO+1 and the HOMO-1 orbitals of the monolayer, since it is quite possible that the HOMO-1 \rightarrow LUMO and HOMO \rightarrow LUMO+1 transitions in the monolayer are in energetic resonance with the S_0 - S_1 transition in the bulk and will thus play a role for the quenching process (see below).

The mechanism which is responsible for the luminescence quenching is most obviously related to the charge transfer from the monolayer to the metal via hybridized molecule-substrate orbitals, leading to fast delocalization of all electronic excitations of the molecules, i.e., the hole in the molecule is rapidly filled by a (resonant) electron transfer from the occupied metal valence band to the molecule, while the electron delocalizes into the unoccupied metallic states. These charge-transfer processes between the monolayer and the substrate are represented by horizontal arrows in Fig. 4. They are especially possible in a planar geometry, as is present here, where the π system is involved in the bonding of the molecule to the metal. The time constant of charge transfer to the metal after the optical excitation can be estimated to be much smaller ($\leq 10^{-12}$ – 10^{-16} s) (Ref. 8) than that of a PL decay ($\sim 10^{-9}$ s).^{33,37} Thus it suppresses the PL of the monolayer most effectively.

The *second* layer is only weakly adsorbed on top of the first layer, although the intermolecular forces between the first and second layer are likely slightly stronger compared to those between higher layers (see above). Nevertheless, effective charge transfer from the second layer to the metal *via tunneling* through the first layer appears to be still possible at this small distance. We note that a relatively high probability for tunneling of electrons through two layers of ordered organic molecules on a metal surface is, e.g., demonstrated by scanning-tunneling microscopy.³⁸ These tunneling processes involving the second layer are also indicated by horizontal lines in Fig. 4. The tunneling transfer rates of charges from

the second layer to the metal are certainly much below those of the first layer, but obviously still high enough to fully suppress the PL of the second layer. We note that such a tunneling process of the excited electron across a spacer layer of fatty acids was also identified from photocurrent measurements on anthracene crystals with evaporated metal electrodes.³⁹

Alternatively to charge transfer, energy transfer may occur, i.e., the exciton may also be transferred from the second to the first layer by Coulombic field coupling (perhaps involving the HOMO-1 or LUMO+1 orbital of the first chemisorbed layer) with subsequent internal conversion of the excess energy and final decay from the first layer (by delocalization of the charges, as discussed above). This is illustrated by the vertical dashed lines in Fig. 4. The importance of a resonant electron transfer as a dominating deexcitation mechanism for molecules in direct contact with a metal surface was also pointed out by Avouris and Persson.⁴⁰ From our data, we cannot discriminate between the transfer rates of Coulombic field coupling and tunneling for the second layer.

The luminescence starts when the *third* layer is deposited. The likely reason is that from the third layer on, the charge-transfer rate is too small to compete significantly with the radiative decay. The steep increase of the PL yield thus reflects the exponential decrease of the tunneling rate with distance from the metal interface.

The proposed mechanism of interface quenching by tunneling and delocalization describes the experimental data well. We demonstrate this for the 4T data using a very simple model. Hereby we assume a constant PL yield (η) for all molecules within d , except for the first two layers (of 7.2 Å total thickness in the case of 4T), where we set $\eta=0$. The averaged PL yield [$\bar{\eta}(d)$] is thus obtained as $\bar{\eta}(d) = (\eta/d) \times (d - 7.2 \text{ Å})$. The computed curve (short-dashed line in Fig. 3) is in good quantitative agreement with our data. In particular, it describes correctly the strong decrease of the PL yield between 30 and 7 Å, and thus clearly supports our model. The description of our data by a model becomes even better if we include exciton diffusion^{41,42} leading to a slightly smaller slope of the curve (full line in Fig. 3), as can be expected.

IV. FINAL CONCLUSIONS AND SUMMARY

Within the scattering of the data points, the simple model of interface quenching, suggested here, gives a fully satisfactory description of the experimental observation. In particular, it correctly describes the quenching in the first two layers and the strong increase of the luminescence rate, if the layer thickness develops from two to about five layers.

One of the most interesting aspects of the proposed quenching mechanism is that it depends specifically on the nonradiative exciton decay rate at the organic/metal interface, the electronic structure of which is related to the surface bonding. Therefore, significant differences are expected for other adsorbate/substrate combinations. In particular, for nonmetallic surfaces, smaller quenching rates should be observed. So far our results *cannot* be interpreted as an indica-

tion that the classical theory is invalid in the few-layer region. They demonstrate, however, that microscopic effects related to the interface bonding and the layer structure of the film are much more relevant for the luminescence quenching in this thickness range. An interesting aspect in this context is that the classical theory predicts a systematic shift of the PL lines as a function of distance to the surface.⁴ However, although we have very narrow vibronic lines here (see Fig. 2), we could not observe any shifts, even for films with thicknesses below 3 ML. The reason for this is not understood yet. One aspect may be that the classical theory so far deals with isolated point dipoles⁴ and not with delocalized excitons in a periodic lattice, as given here. An obvious consequence of our finding is that luminescence detection of π -conjugated molecules in the planar adsorption geometry on metal surfaces is impossible for the first two layers, but may be possible to perform with a sufficient signal-to-noise ratio from the third layer onward. This result should be, e.g., considered for experiments aiming at the luminescence detection of single molecules on metal surfaces. In a recent experiment, luminescence of porphyrines adsorbed on Cu(100) could be induced by a scanning tunneling micro-

scope tip.⁴⁴ However, in this experiment the central π system was sterically decoupled from the Cu surface by “legs” of di-*t*-butylphenyl groups. Therefore, the situation is different with respect to that considered here; the observation of luminescence in the latter case does not contradict our results.

In summary, we have shown that structurally highly ordered thin films of planar π -conjugated molecules on the Ag(111) surface do not luminescence for thicknesses below two completed molecular layers. The luminescence quenching presumably occurs by an ultrafast nonradiative decay of excitons by a charge-transfer mechanism at the organic/metal interface which is effective for the *first chemisorbed and the second* molecular layer. From the third layer the luminescence yield increases steeply.

ACKNOWLEDGEMENTS

We are grateful to the Deutsche Forschungsgemeinschaft for financial support (Um 6/4-2, 4-3), Dr. P. Feulner for helpful comments, and Professor A. Forchel for the loan of equipment. One of us (E.U.) gratefully acknowledges support by the Fonds der Chemischen Industrie.

*Corresponding author. Email address: sokolowski@thch.uni-bonn.de

¹K. H. Drexhage, M. Fleck, H. Kuhn, F. P. Schäfer, and W. Sperling, *Ber. Bunsenges. Phys. Chem.* **73**, 1179 (1969).

²For a review, see *Semiconducting Polymers—Chemistry, Physics and Engineering*, edited by G. Hadziioannou and P. F. van Hutten (Wiley-VCH, Weinheim, 1999).

³E. Umbach, M. Sokolowski, and R. Fink, *Appl. Phys. A: Mater. Sci. Process.* **63**, 565 (1996).

⁴R. R. Chance, A. Prock, and R. Silbey, in *Advances in Chemical Physics*, edited by I. Prigogine and S. A. Rice (Wiley Interscience, New York, 1978), Vol. 37, p. 1.

⁵D. H. Waldeck, A. P. Alivisatos, and C. B. Harris, *Surf. Sci.* **158**, 103 (1984).

⁶M. Daffertshofer, H. Port, and H. C. Wolf, *Chem. Phys.* **200**, 225 (1995).

⁷A. Rosenberg and D. L. Peebles, *Chem. Phys. Lett.* **234**, 221 (1995).

⁸Ph. Avouris and J. Demuth, *J. Chem. Phys.* **75**, 4783 (1981).

⁹U. Gómez, M. Leonardt, H. Port, and H. C. Wolf, *Chem. Phys. Lett.* **268**, 1 (1997).

¹⁰M. Leonardt, O. Mager, and H. Port, *Chem. Phys. Lett.* **313**, 24 (1999).

¹¹R. Scholz, I. Vragovic', A. Y. Kobitski, M. Schreiber, H. P. Wagner, and D. R. T. Zahn, *Phys. Status Solidi B* **234**, 402 (2002).

¹²M. Schneider, Doctoral thesis, Universität Würzburg (2002); M. Schneider, M. Sokolowski, and E. Umbach (unpublished).

¹³W. Gebauer, M. Bäessler, R. Fink, M. Sokolowski, and E. Umbach, *Chem. Phys. Lett.* **266**, 177 (1997).

¹⁴A. Soukopp, C. Seidel, R. Li, M. Bäessler, M. Sokolowski, and E. Umbach, *Thin Solid Films* **284**, 343 (1996).

¹⁵M. Jung, U. Baston, G. Schnitzler, M. Kaiser, J. Papst, T. Porwol, H. J. Freund, and E. Umbach, *J. Mol. Struct.* **293**, 239 (1993).

¹⁶J. Taborski, P. Väterlein, H. Dietz, U. Zimmermann, and E. Umbach, *J. Electron Spectrosc. Relat. Phenom.* **75**, 129 (1995).

¹⁷R. Li, P. Bäuerle, and E. Umbach, *Surf. Sci.* **331-333**, 100 (1995).

¹⁸E. Umbach, W. Gebauer, A. Soukopp, M. Bäessler, and M. Sokolowski, *J. Lumin.* **76**, 641 (1998).

¹⁹V. Shklover, F. S. Tautz, R. Scholz, S. Sloboshanin, M. Sokolowski, J. A. Schaefer, and E. Umbach, *Surf. Sci.* **454**, 60 (2000).

²⁰L. Kilian, Doctoral thesis, Universität Würzburg (2002); L. Kilian, E. Umbach, M. Sokolowski (unpublished).

²¹V. Wagner, T. Muck, J. Geurts, M. Schneider, and E. Umbach, *Appl. Surf. Sci.* **212-213**, 520 (2003).

²²The revised thickness calibration used here differs by a factor of 1.2 with respect to that in Ref. 21, where the thickness of the individual layers was slightly underestimated.

²³K. Glöckler, C. Seidel, A. Soukopp, M. Sokolowski, E. Umbach, M. Böhringer, R. Berndt, and W.-D. Schneider, *Surf. Sci.* **405**, 1 (1998).

²⁴B. Krause, A. C. Dürr, K. A. Ritley, F. Schreiber, H. Dosch, and D. Smilgies, *Appl. Surf. Sci.* **175**, 332 (2001).

²⁵S. R. Forrest, L. Y. Leu, F. F. So, and W. Y. Yoon, *J. Cryst. Growth* **66**, 5908 (1989); M. Möbus, N. Karl, and T. Kobayashi, *J. Cryst. Growth* **116**, 495 (1992).

²⁶T. Schmidt, R. Fink, and E. Umbach (unpublished results).

²⁷C. Seidel, A. Soukopp, R. Li, P. Bäuerle, and E. Umbach, *Surf. Sci.* **374**, 17 (1997).

²⁸D. Birnbaum, D. Fichou, and B. E. Kohler, *J. Chem. Phys.* **96**, 165 (1992).

²⁹M. Muccini, M. Schneider, C. Taliani, M. Sokolowski, E. Umbach, D. Beljonne, J. Cornil, and J. L. Bredas, *Phys. Rev. B* **62**, 6296 (2000).

³⁰A. Langner, W. Gebauer, M. Sokolowski, and E. Umbach (unpublished).

³¹The reflectivity was estimated from the Fresnel formula using $\epsilon_{Ag} = (0.05 + 2.1i)^2$,³² $\epsilon_{4T} = (2 + 0.8i)^2$.³³

³²P. B. Johnson and R. W. Christy, *Phys. Rev. B* **6**, 4370 (1972).

³³H.-J. Egelhaaf, Doctoral thesis, Universität Tübingen (1996).

- ³⁴B. N. J. Persson and N. D. Lang, Phys. Rev. B **26**, 5409 (1982).
³⁵P. M. Whitmore, H. J. Robota, and C. B. Harris, J. Chem. Phys. **77**, 1560 (1982).
³⁶See, e.g., *Desorption Induced by Electronic Transitions, DIET II*, edited by W. Brenig and D. Menzel (Springer, Berlin, 1985); *Desorption Induced by Electronic Transitions, DIET IV*, edited by G. Betz and P. Varga (Springer, Berlin, 1990).
³⁷M. Hopmeier, W. Gebauer, M. Oestreich, M. Sokolowski, E. Umbach, and R. F. Mahrt, Chem. Phys. Lett. **99**, 314 (1999).
³⁸E. Umbach, K. Glöckler, and M. Sokolowski, Surf. Sci. **402**, 20 (1998).
³⁹H. Killesreiter and H. Bässler, Chem. Phys. Lett. **11**, 411 (1971).
⁴⁰P. Avouris and B. Persson, J. Phys. Chem. **88**, 837 (1984).
⁴¹For mathematical details, see also Z. Ophir, N. Schwentner, B. Raz, M. Skibowski, and J. Jortner, J. Chem. Phys. **63**, 1072 (1975).
⁴²In our *nonclassical model* we used the most simple approximations $k_{\text{nonrad}} + k_{\text{rad}} = \text{const}$ (decay rate independent of z) and $\eta(z) = k_{\text{rad}} / (k_{\text{nonrad}} + k_{\text{nonrad}}) = \text{const} = \eta$ (PL yield independent of z). The general solution for the exciton density $n(z)$ for this case can be found, e.g., in Ref. 41. Our model assumes that $n(z) = 0$ for the first two monolayers due to the postulated ultrafast quenching process at the interface. Thus we used the boundary conditions $n[z = z_0 = d(2 \text{ ML}) = 7.2 \text{ \AA}] = 0$ and

$n(z \rightarrow \infty) = \text{const}$. This yields

$$n(z) \propto \left[1 - \exp\left(-\frac{z - z_0}{\sqrt{D(k_{\text{nonrad}} + k_{\text{rad}})}}\right) \right],$$

where $z_0 = 7.2 \text{ \AA}$. Equation (1) has to be modified in this case to give

$$\begin{aligned} \bar{\eta}(d) &= \frac{1}{d} \int_0^d n(z) \eta(z) dz \\ &= \frac{1}{d} \int_{z_0}^d n(z) \frac{k_{\text{radiative}}}{k_{\text{radiative}} + k_{\text{nonradiative}}} dz \\ &= \frac{1}{d} \int_{z_0}^d n(z) \eta dz. \end{aligned}$$

The resulting curve calculated for $\bar{\eta}(d)$ including diffusion ($D = 10^{-5} \text{ cm}^2 \text{ s}^{-1}$) is shown in Fig. 3 as the full line [$D = 10^{-5} \text{ cm}^2 \text{ s}^{-1}$ (Ref. 43)].

- ⁴³E. A. Silinsh and V. Čápek, *Organic Molecular Crystals, Interaction, Localization and Transport Phenomena* (AIP Press, Woodbury, NY, 1994).
⁴⁴W. Deng, D. Fujita, T. Ohgi, S. Yokoyama, K. Kamikado, and S. Mashiko, J. Chem. Phys. **117**, 4995 (2002).